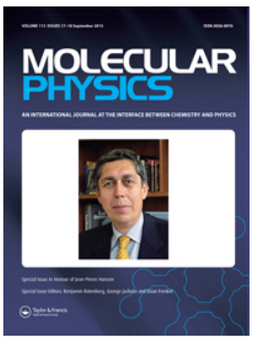

Taylor & Francis
Taylor & Francis Group

Molecular Physics

An International Journal at the Interface Between Chemistry and Physics

ISSN: 0026-8976 (Print) 1362-3028 (Online) Journal homepage: http://www.tandfonline.com/loi/tmph20

Effective interactions of DNA-stars

Clara Abaurrea Velasco, Christos N. Likos & Gerhard Kahl

To cite this article: Clara Abaurrea Velasco, Christos N. Likos & Gerhard Kahl (2015) Effective interactions of DNA-stars, Molecular Physics, 113:17-18, 2699-2706, DOI: 10.1080/00268976.2015.1048318

To link to this article: https://doi.org/10.1080/00268976.2015.1048318

Molecular Physics, 2015
Vol. 113, Nos. 17–18, 2699–2706, http://dx.doi.org/10.1080/00268976.2015.1048318

Taylor & Francis
Taylor & Francis Group

INVITED ARTICLE

Effective interactions of DNA-stars

Clara Abaurrea Velasco[a,b], Christos N. Likos[c] and Gerhard Kahl[a,*]

[a]*Institute for Theoretical Physics and Center for Computational Materials Science (CMS), TU Wien, Wiedner Hauptstraße 8-10, A-1040 Vienna, Austria;* [b]*Theoretical Soft Matter and Biophysics, Institute of Complex Systems and Institute for Advanced Simulation, Jülich, Germany;* [c]*Faculty of Physics, University of Vienna, Boltzmanngasse 5, A-1090 Vienna, Austria*

(*Received 20 February 2015; accepted 21 April 2015*)

We put forward a model that allows the calculation of the effective potential of two interacting DNA-stars, i.e., three-armed, Y-shaped, charged macromolecules, built up by three intertwined single-stranded DNAs. These particles are assumed to float on a flat interface separating two media with different dielectric properties. As the only input, our model requires the charge density along the branches and the interaction between two infinitesimally short segments, along two interacting rods. With this effective interaction at hand, a detailed investigations of the self-assembly scenarios of these molecules either via computer simulations or via theoretical frameworks comes within reach.

Keywords: effective interactions; DNA-stars

1. Introduction

Dendrimers are tree-like, highly branched macromolecules with a regular internal architecture. These macromolecules are synthesised in a step-wise process where – starting from a central, multi-functional core – branched units are added repeatedly. The number of theoretical and experimental investigations dedicated to these particles has seen a remarkable increase during the past years, a fact which is due to the particular role of dendrimers in possible applications [1], which include their roles as solubility enhancement [2], as drug-delivery vectors [3,4], as nanocarriers [5], and many more. Most investigations on dendrimers have been dedicated to neutral molecules, while considerably less is known about their charged counterparts. Charging dendrimers offer additional possibilities of responsiveness of these macromolecules to external stimuli, such as the pH, salinity and electric fields; accordingly, their conformations and interactions can be tuned in a variety of ways [6,7]. Such features are of relevance when these macromolecules are expected to self-assemble in a well-defined manner into target structures. Simulation studies have revealed that charged dendrimers form crystals at large values of the electrostatic screening lengths, which melt at lower values of the same [8,9]. This is in agreement with experimental findings [10].

An obvious building block for such charged dendrimers are double-stranded DNAs (dsDNAs) which indeed have been used for this purpose in recent investigations: a few years ago Luo *et al.* [11] succeeded to synthesise in a controlled fashion dendrimer-like DNAs via an enzymatic ligation of basic, branched units; they are referred to as Y-shaped DNAs or DNA-stars. They are formed by three intertwined single-stranded DNAs (ssDNAs), resulting into a Y-shaped nanomolecule with each of its three branches being a dsDNA. Each arm consists of 13 base pairs and thus has a length of about 4.4 nm, slightly exceeding the pitch height of the dsDNA. Such a length corresponds to less than 10% of the persistence length of the dsDNA, thus we can safely assume that the arms of the DNA-stars are rather stiff. The properties of DNA-stars have been investigated both in theory and in experiment in three- and two-dimensional systems. In the latter case, a standard set-up is that they float on a flat interface that separates two media (typically air and a microscopic solvent).

In an effort to obtain a deeper insight into the self-assembly strategies of such DNA-stars, one has to first understand on a quantitative level their interaction properties. In this contribution, we propose a model that allows to calculate the effective potential of two interacting DNA-stars that float on a flat interface that separates two media (with possibly different dielectric properties). Within this formalism, we assume that the charge density along each of the branches of the two interacting stars is the same and that two segments along these two branches (arms) interact via a suitable potential. With these two ingredients at hand, we are able to derive an expression for the effective potential of two interacting stars whose centres are separated by a vector $\mathbf{R}$ and who are tilted with respect to each other by an angle θ.

The manuscript is organised as follows: in the subsequent section, we present the model and construct, starting from the charge densities along the branches, the effective

* Corresponding author. Email: gerhard.kahl@tuwien.ac.at

potential of two interacting DNA-stars; specific models for the charge densities and for the potentials that specify the interaction of two infinitesimal segments of two interacting rods are presented. Results are discussed for particular models in Section 3 and the manuscript is closed with concluding remarks and an outlook.

2. Model

2.1. General remarks on the model

We consider a system of DNA-stars that float on a flat interface, separating two media (specified by indices I and II and, possibly, characterised by different dielectric constants, ε_{I} and $\varepsilon_{\mathrm{II}}$). For the DNA-stars, we assume (1) that their three branches are stiff and identical in their internal architecture and (2) that the angle enclosed by two arms (rods) is fixed at 120°. The validity of these assumptions is easily verified by the considerations put forward in Section 1.

DNA is a polyelectrolyte, as the phosphate groups on the double-helix strands dissociate in water leaving behind electrically charged repeat units and counterions in the solution. At the same time, (salt) counterions recondense on the DNA-rods in ways that are specific to the condensing agents. In particular, whereas salts with Mn^{+2}, Cd^{+2}, sperimidine, protamine or cobalt hexammine condense preferentially into the DNA-grooves, other counterions, such as Ca^{+2} of Mg^{+2} have affinity to the phosphates and adsorb on the DNA-strands. The net effect is a reduction of the bare charge per pitch of the DNA. Thereby, a linearised theory of screening of the (reduced) bare DNA-charge is physically justified, and an analytical solution has been put forward for the full helical DNA-charge distribution by Kornyshev and Leikin [12,13]. This screened electrostatic potential has subsequently been employed to explain the self-assembly of columnar DNA-aggregates on a variety of experimentally observed structures [14,15].

The Konryshev–Leikin potential brings forward a very interesting coupling between the translation of DNA-parallel segments and the rotation around their axes *along* the cylinder. For the problem at hand, however, in which the Y-DNA junctions are lying flat on the water–air interface, the rods are not parallel; moreover, they cannot rotate around their long axes, since each rod in the Y-junction is hindered by the presence of the other two. Accordingly, it is meaningful to ignore the helical charge distribution along the DNA-rods and model the latter as uniformly charged, and composed of elementary segments that interact with one another via a Yukawa potential.

We now proceed to the calculation of the effective potential energy $V_{\mathrm{eff}}^{\mathrm{ss}}(\mathbf{R},\theta)$ of two DNA-stars, whose centres are separated by a two-dimensional vector $\mathbf{R} = (R_x, R_y)$ and that are tilted with respect to each other by an angle θ (see Figure 1). This task can be reduced to calculate

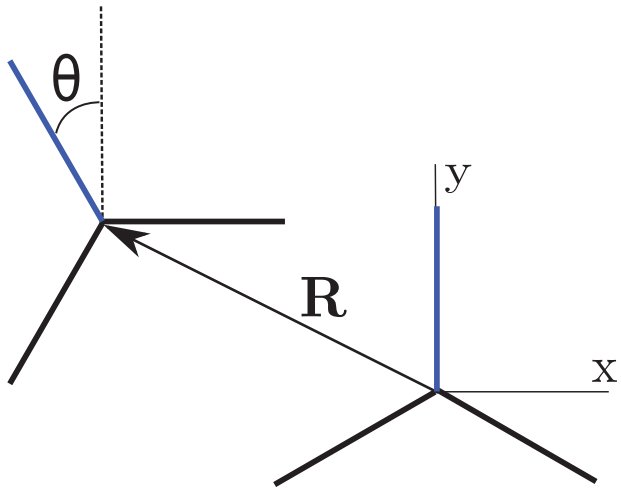

Figure 1. Schematic view of two interacting DNA-stars. For simplicity, the centre of the first one is located in the origin of the Cartesian coordinate system, with one of its arm pointing in the positive y-direction; the other star, whose centre is connected to the centre of the former one by the vector $\mathbf{R}$ is tilted with respect to the first star via an angle θ in counter-clockwise orientation. One branch of each star is highlighted in blue, specifying those rods for which the effective rod–rod interaction $V_{\mathrm{eff}}^{\mathrm{rr}}(\mathbf{R},\theta)$ is calculated (see text).

first the effective potential energy $V_{\mathrm{eff}}^{\mathrm{rr}}(\mathbf{R},\theta)$ of two rods (to be labelled by indices 1 and 2), each of them belonging to one of the interacting stars; these branches (rods) are again separated by the two-dimensional vector $\mathbf{R}$ and are tilted with respect to each other by the angle θ. The total star–star potential $V_{\mathrm{eff}}^{\mathrm{ss}}(\mathbf{R},\theta)$ is then obtained by the superposition of respective rod–rod potentials, taking into account the mutual orientations of the 2×3 branches. The final result for $V_{\mathrm{eff}}^{\mathrm{ss}}(\mathbf{R},\theta)$ will be presented in Subsection 2.4.

Let us assume that the (charge) densities along rods 1 and 2 are specified by $\rho^{(1)}_{\mathbf{0},\theta=0}(\mathbf{r})$ and $\rho^{(2)}_{\mathbf{R},\theta}(\mathbf{r})$, with $\mathbf{r} = (x, y)$ being a two-dimensional vector; for simplicity, we have assumed that rod 1 is oriented along the y-axis, with one of its end being located in the origin of the coordinate system (see Figure 1, where all the relevant variables are specified). For clarification, we emphasise that henceforward the first (vector) index of the densities refers to the vector, pointing from the origin of the Cartesian coordinate system to the tip of the respective rod, while the second index specifies the rotation angle of this rod with respect to the y-axis (in a counter-clockwise orientation). At this point, we also clarify that the rods can overlap, i.e., we do not include steric interactions; this assumption drastically reduces the complexity of the problem.

Due to simple geometric considerations, the following relation holds:

$$\rho_{\mathbf{R},\theta}(\mathbf{r}) = \rho_{\mathbf{0},\theta}(\mathbf{r}-\mathbf{R}) = \rho_{\mathbf{0},0}\left[\mathcal{R}(\theta)\cdot(\mathbf{r}-\mathbf{R})\right], \qquad (1)$$

with $\mathcal{R}(\theta)$ being the usual two-dimensional matrix that specifies a counter-clockwise rotation via the angle θ,

$$\mathcal{R}(\theta) = \begin{pmatrix} \cos\theta & -\sin\theta \\ \sin\theta & \cos\theta \end{pmatrix}$$
$$\mathcal{R}^{-1}(\theta) = \begin{pmatrix} \cos\theta & \sin\theta \\ -\sin\theta & \cos\theta \end{pmatrix}. \quad (2)$$

For simplicity, the argument of $\mathcal{R}$ will be dropped henceforward. Possible functional forms for the $\rho^{(i)}_{\mathbf{0},0}(\mathbf{r})$ will be discussed in Subsection 2.2.

Furthermore, we assume that two infinitesimal segments located at positions $\mathbf{r}_1$ and $\mathbf{r}_2$ on either of the rods interact via a potential $\Phi(|\mathbf{r}_1 - \mathbf{r}_2|)$; for possible functional forms of this potential, we refer to Subsection 2.3.

With these assumptions, $V^{\mathrm{rr}}_{\mathrm{eff}}(\mathbf{R}, \theta)$ is given by

$$V^{\mathrm{rr}}_{\mathrm{eff}}(\mathbf{R}, \theta) = \int \mathrm{d}^2 r_1 \mathrm{d}^2 r_2 \; \rho^{(1)}_{\mathbf{0},0}(\mathbf{r}_1)\Phi(|\mathbf{r}_1 - \mathbf{r}_2|)\rho^{(2)}_{\mathbf{R},\theta}(\mathbf{r}_2). \quad (3)$$

For convenience, we introduce the Fourier-transform, $\tilde{f}(\mathbf{k})$, of a function $f(\mathbf{r})$ via

$$\tilde{f}(\mathbf{k}) = \frac{1}{2\pi}\int \mathrm{d}^2 r \; f(\mathbf{r})\mathrm{e}^{-\mathrm{i}\mathbf{k}\cdot\mathbf{r}}$$
$$f(\mathbf{r}) = \frac{1}{2\pi}\int \mathrm{d}^2 k \; \tilde{f}(\mathbf{k})\mathrm{e}^{\mathrm{i}\mathbf{k}\cdot\mathbf{r}}, \quad (4)$$

where i is the complex unit.

Using Equation (1), we obtain

$$\tilde{\rho}_{\mathbf{R},\theta}(\mathbf{k}) = \frac{1}{2\pi}\int \mathrm{d}^2 r \; \rho_{\mathbf{R},\theta}(\mathbf{r})\mathrm{e}^{\mathrm{i}\mathbf{k}\cdot\mathbf{r}} \quad (5)$$
$$= \frac{1}{2\pi}\int \mathrm{d}^2 r \; \rho_{\mathbf{0},0}\left[\mathcal{R}\cdot(\mathbf{r}-\mathbf{R})\right]\mathrm{e}^{\mathrm{i}\mathbf{k}\cdot\mathbf{r}} \quad (6)$$
$$= \frac{1}{2\pi}\int \mathrm{d}^2 r \; \rho_{\mathbf{0},0}\left[\mathcal{R}\cdot(\mathbf{r}-\mathbf{R})\right]\mathrm{e}^{\mathrm{i}\mathbf{k}\cdot(\mathbf{r}-\mathbf{R})}\mathrm{e}^{\mathrm{i}\mathbf{k}\cdot\mathbf{R}} \quad (7)$$
$$= \frac{1}{2\pi}\int \mathrm{d}^2 r \; \rho_{\mathbf{0},0}\left[\mathcal{R}\cdot(\mathbf{r}-\mathbf{R})\right]\mathrm{e}^{\mathrm{i}\mathbf{k}\cdot\mathcal{R}^{-1}\cdot\mathcal{R}\cdot(\mathbf{r}-\mathbf{R})}\mathrm{e}^{\mathrm{i}\mathbf{k}\cdot\mathbf{R}} \quad (8)$$
$$= \tilde{\rho}_{\mathbf{0},0}(\mathbf{k}\cdot\mathcal{R}^{-1})\mathrm{e}^{\mathrm{i}\mathbf{k}\cdot\mathbf{R}}, \quad (9)$$

with $\mathbf{k}\cdot\mathcal{R}^{-1} = (k_x\cos\theta - k_y\sin\theta, k_x\sin\theta + k_y\cos\theta)$.

Introducing the Fourier-transforms of the respective factors in the convolution integral (3), the Fourier-transform of $V^{\mathrm{rr}}_{\mathrm{eff}}(\mathbf{R}, \theta)$ can be expressed via

$$\tilde{V}^{\mathrm{rr}}_{\mathrm{eff}}(\mathbf{k}, \theta) = \tilde{\rho}^{(1)}_{\mathbf{0},0}(\mathbf{k})\tilde{\Phi}(\mathbf{k})\tilde{\rho}^{(2)}_{\mathbf{0},\theta}(-\mathbf{k}). \quad (10)$$

2.2. Models for the charge density

In the simplest model for the charge density (specified by the label A), we assume that this function is constant and that the rods of length L are infinitely thin, thus

$$\rho^{[\mathrm{A}]}_{\mathbf{0},0}(\mathbf{r}) = \frac{1}{L}\delta(x)\Theta(y)\Theta(L-y)$$
$$= \frac{1}{L}\delta(x)\Theta\left(\frac{L}{2} - \left|y - \frac{L}{2}\right|\right). \quad (11)$$

In model B, we assume again that the charge density is constant and we attribute a finite value D to the thickness of the rods, thus

$$\rho^{[\mathrm{B}]}_{\mathbf{0},0}(\mathbf{r}) = \frac{1}{LD}\Theta\left(\frac{D}{2} - |x|\right)\Theta(y)\Theta(L-y)$$
$$= \frac{1}{LD}\Theta\left(\frac{D}{2} - |x|\right)\Theta\left(\frac{L}{2} - \left|y - \frac{L}{2}\right|\right). \quad (12)$$

The respective Fourier-transforms are given by

$$\tilde{\rho}^{[\mathrm{A}]}_{\mathbf{0},0}(\mathbf{k}) = Ze\frac{1}{2\pi L}\frac{\mathrm{i}}{k_y}\left[\mathrm{e}^{-\mathrm{i}k_y L} - 1\right] \quad (13)$$

and

$$\tilde{\rho}^{[\mathrm{B}]}_{\mathbf{0},0}(\mathbf{k}) = Ze\frac{1}{\pi LD}\frac{\mathrm{i}}{k_x k_y}\sin\left(\frac{Dk_x}{2}\right)\left[\mathrm{e}^{-\mathrm{i}k_y L} - 1\right]. \quad (14)$$

2.3. Models for the interaction kernels

In case that both media have the same dielectric constants, ε, $\Phi(r)$ and its Fourier-transform, $\tilde{\Phi}(k)$, are given by

$$\Phi(r) = \frac{Ze}{\varepsilon}\frac{\mathrm{e}^{-\kappa r}}{r} \quad \tilde{\Phi}(k) = \frac{Ze}{\varepsilon}\frac{1}{\sqrt{\kappa^2 + \mathbf{k}^2}}, \quad (15)$$

Z being the charge of the line segment, e being the elementary charge and κ being the inverse Debye screening length.

In case that the interface separates two media (characterised by the dielectric constants ε_{I} and $\varepsilon_{\mathrm{II}}$), $\tilde{\Phi}(k)$ is given by [16]

$$\tilde{\Phi}(k) = 2Ze\frac{1}{\varepsilon_{\mathrm{I}}\sqrt{\kappa_{\mathrm{I}}^2 + \mathbf{k}^2} + \varepsilon_{\mathrm{II}}\sqrt{\kappa_{\mathrm{II}}^2 + \mathbf{k}^2}}, \quad (16)$$

κ_{I} and κ_{II} being the screening parameters of the respective media.

2.4. The total effective interaction

With the appropriate choices for $\rho^{(i)}_{\mathbf{0},0}(\mathbf{r})$, $i = 1, 2$ and for $\Phi(\mathbf{r})$, the Fourier-transform of the rod–rod interaction,

$\tilde{V}^{\mathrm{rr}}_{\mathrm{eff}}(\mathbf{k}, \theta)$, can be calculated via Equation (10); the corresponding expression in r-space is obtained via an inverse Fourier-transform.

Finally, we obtain the Fourier-transform of the effective star–star potential, $V^{\mathrm{ss}}_{\mathrm{eff}}(\mathbf{R}, \theta)$, by summing up over the interactions of the 2×3 rods that form the stars

$$V^{\mathrm{ss}}_{\mathrm{eff}}(\mathbf{R}, \theta) = 3 \sum_{j=0,1,2} V^{\mathrm{rr}}_{\mathrm{eff}}(\mathbf{R}, \theta + 2\pi j/3). \qquad (17)$$

At this point it should be emphasised that both our models for the interaction kernels are based on a linear, Debye–Hückel-like concept. This approach might righteously be debated as it is definitely not valid if the potential between segments of the DNA-strands are strong; in this case, the use of the full Poisson–Boltzmann equation is unavoidable.

For simplicity, we have assumed in the present contribution that the interactions between DNA-segments are not too strong, taking thus the benefit of the availability of analytic expressions. However, we emphasise that our simplified, linear approach is able to capture on a qualitative level also the features of a potential that is calculated via the full, nonlinear approach. In particular, our approach is realistic in the following sense: (1) even the full, nonlinear

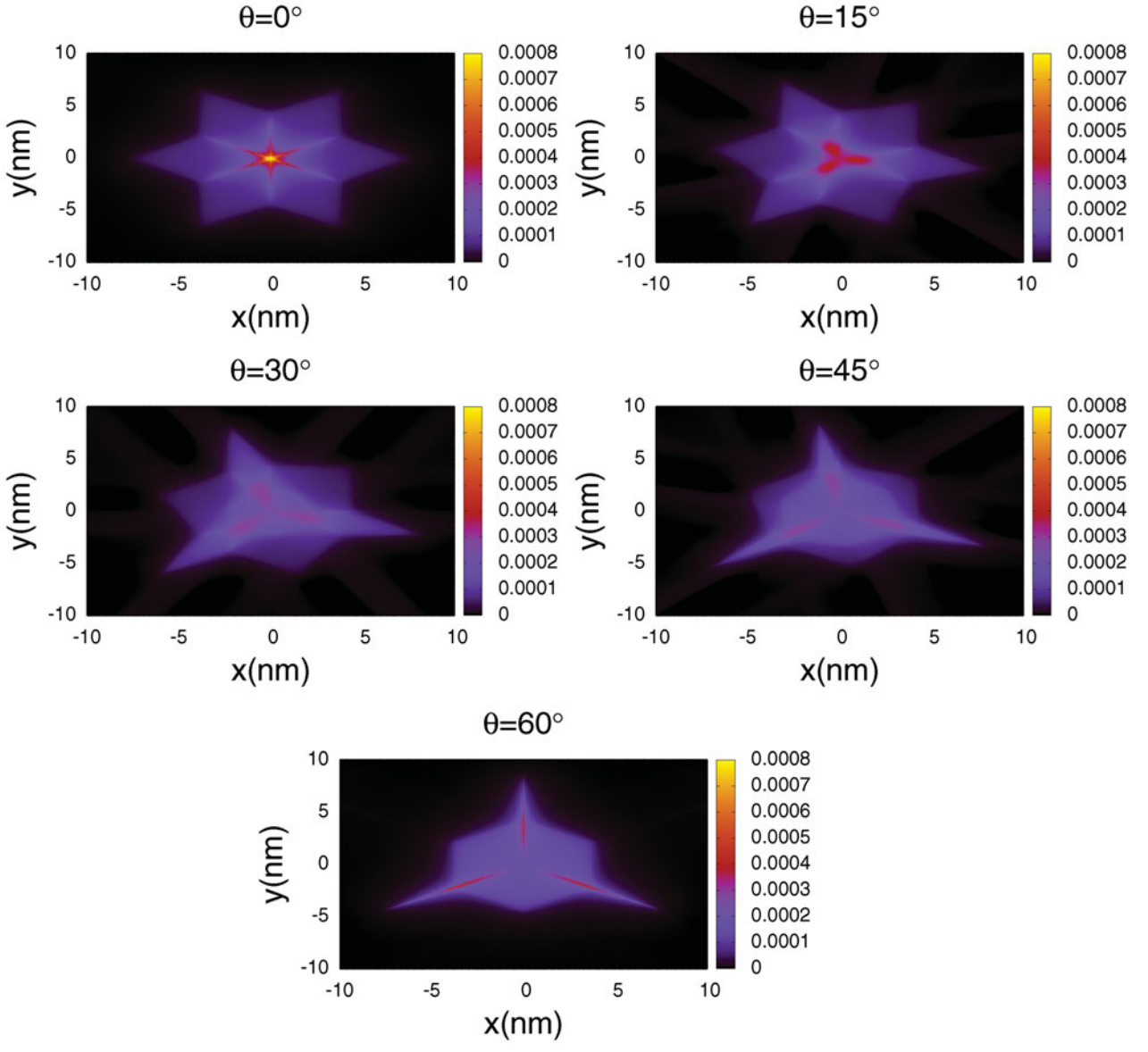

Figure 2. Contour plots of the effective star–star potential, $V^{\mathrm{ss}}_{\mathrm{eff}}(\mathbf{R}, \theta)$, for two interacting DNA-stars in arbitrary units: the centre of the first one is located in the origin of the Cartesian coordinate system and one of its branches is oriented in the positive y-direction; the centre of the second star is located at a position $\mathbf{R} = (x, y)$ and is tilted with respect to the first one via an angle θ in a counter-clockwise orientation; panels show results for selected θ-values (as labelled at the top of each panel). The colour scale for the potential is given at the right-hand side of each panel. x- and y-values are given in nm, κ is chosen to be 1 nm^{-1}. The length of the infinitely thin rods is chosen to be 4.42 nm and no mismatch in the dielectric properties of the two media is assumed.

potential has a Yukawa-like decay due to salt screening; (2) the coupling between the orientational and translational dependence is faithfully reproduced; and (3) introducing a suitably defined 'renormalised charge' in the linearised approximation, the two approaches can be matched. In particular, the renormalised charge can be used as input instead of the bare charge to implicitly account for nonlinear effects, see, e.g., [17].

3. Results

3.1. Numerical details

At this point, a few remarks on the numerics are in order. The effective rod–rod potential in real space was obtained via a numerical Fourier-transform of $\tilde{V}_{\text{eff}}^{\text{rr}}(\mathbf{k}, \theta)$. This was achieved with a two-dimensional Fast-Fourier-algorithm using 1024 grid points in the two orthogonal directions with a grid-size in k space of $\Delta k_x = \Delta k_y = 0.05$; these values correspond to $\Delta x = \Delta y = 0.1227$.

3.2. The effective potentials

Data obtained for the effective potentials are summarised for four different models in Figures 2–5: we first consider a system where both media have the same dielectric properties, assuming branches that are either infinitely thin or of finite thickness (Figures 2 and 3, respectively); then we consider the situation that the interface separates water from air, focusing again the two cases of branch thickness (Figures 4 and 5, respectively).

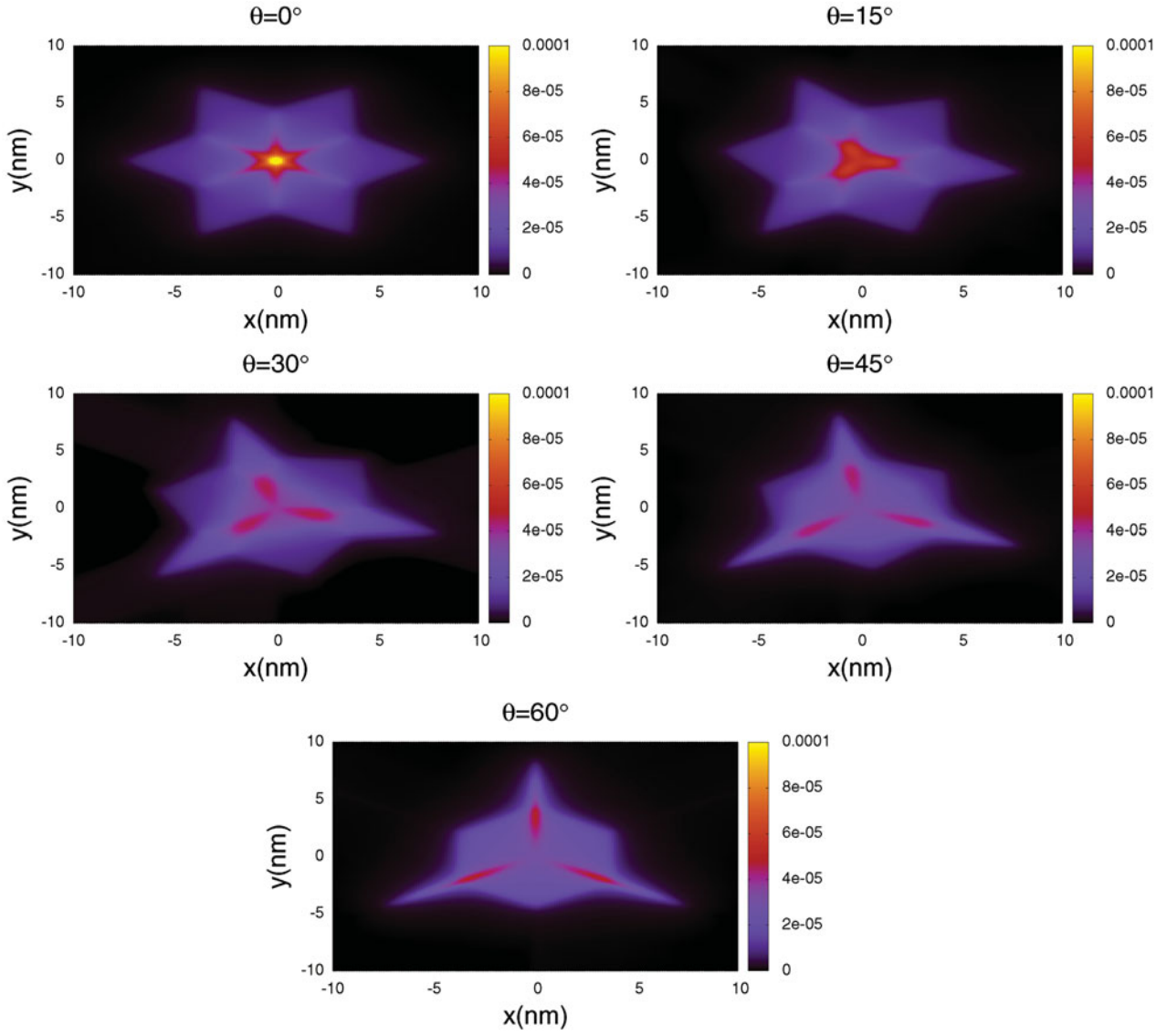

Figure 3. Results for $V_{\text{eff}}^{\text{ss}}(\mathbf{R}, \theta)$ in a representation similar to the one as in Figure 2. In this systems, the rods are of finite thickness, corresponding to 1/9 of the rod-length and no mismatch in the dielectric properties of the two media is assumed.

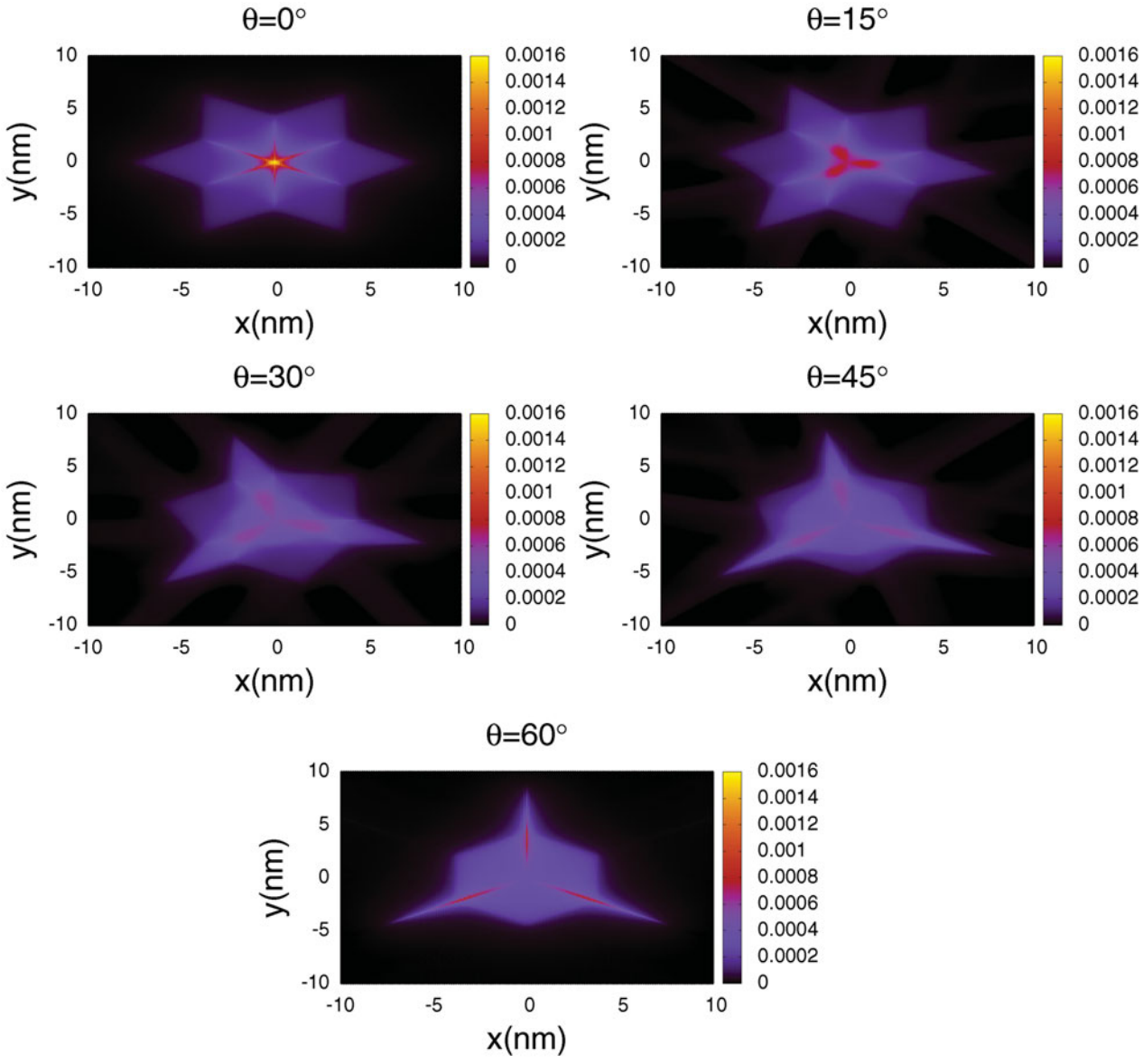

Figure 4. Results for $V_{\text{eff}}^{\text{ss}}(\mathbf{R}, \theta)$ in a representation similar to the one as in Figure 2. In this system, the rods are infinitely thin and it is assumed that the interface separates air from water (with $\varepsilon_{\text{II}} = 78$); $\kappa_I = 0$, while $\kappa_{\text{II}} = 1$ nm^{-1}.

For the presentation of the effective potential $V_{\text{eff}}^{\text{rr}}(\mathbf{r}, \theta)$ of two interacting DNA-stars, we have assumed that the centre of the first one is located in the origin of the two-dimensional Cartesian coordinate system, with one of its branches oriented in the positive y-direction. The centre of the second DNA-star is located at some point $\mathbf{R} = (x, y)$ and the molecule is tilted with respect to the first one via an angle θ in a counter-clockwise orientation. Due to the internal symmetry of the problem it is sufficient to consider only θ-values with $\theta \in [0^{\text{o}}, 60^{\text{o}}]$. The fact that the effective potential depends on three arguments forced us to present the data in the following, selective way: in each panel of the four figures, the effective potential is shown in a contour plot in the (x, y)-plane (each point representing a possible location for the centre of the second DNA-star) for a selected θ-value; in total five θ-values have been considered: $\theta = 0^{\text{o}}$, 15^{o}, 30^{o}, 45^{o} and 60^{o}. At this point it should be emphasised that at a particular position (specified by an x- and a y-value), the respective value of $V_{\text{eff}}^{\text{rr}}(\mathbf{r}, \theta)$ represents the total interaction energy experience by the stars.

A first, qualitative inspection of these figures shows that the general pattern of these contour plots is very similar for all four systems considered. Two main trends can be identified: (1) as we pass from infinitely thin rods to branches of finite thickness, the rather sharp pattern of the former case becomes blurred and softened; (2) as we introduce a mismatch in the dielectric properties of the two media, the

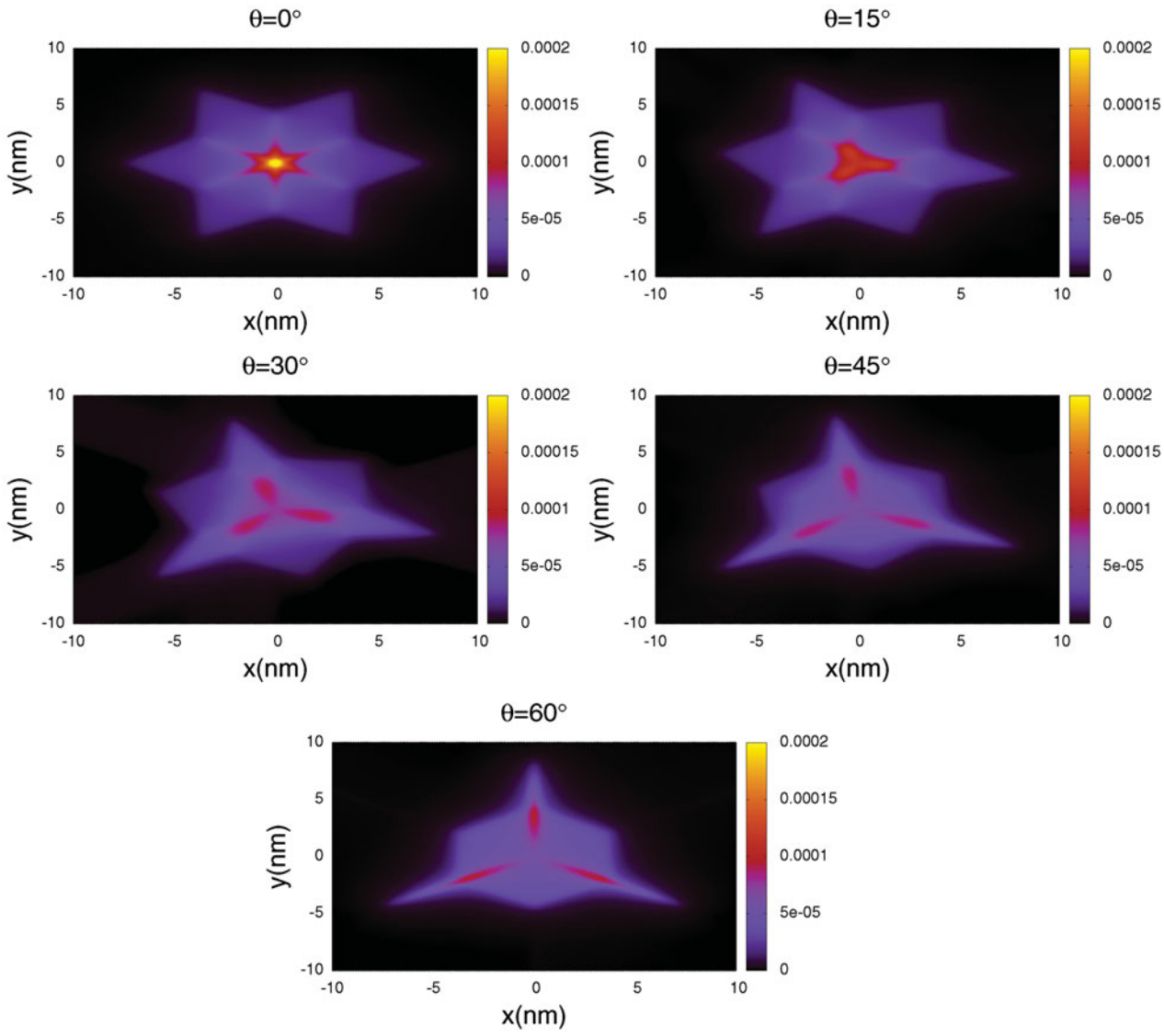

Figure 5. Results for $V_{\text{eff}}^{\text{ss}}(\mathbf{R}, \theta)$ in a representation similar to the one as in Figure 4. In this system the rods are finite thickness (corresponding to 1/9 of the rod-length) and it is assumed that the interface separates air from water (with $\varepsilon_{\text{II}} = 78$); $\kappa_I = 0$, while $\kappa_{\text{II}} = 1\ \text{nm}^{-1}$.

strength of the potential is roughly increased by a factor of two, demonstrating the strong influence of the dielectric properties on the effective interactions.

Throughout we observe in each of the panels a more or less distorted area, reminiscent of a six-tipped star; outside this region the stars do not experience any interaction (coloured in black in the panels). The complex colour distribution inside these regions provide evidence of an intricate spatial and orientational dependence of the effective interactions. At $\theta = 0^{\text{o}}$, the range where the interaction does not vanish is a symmetric star; the potential assumes at the origin a very high value, where the two stars fully overlap; furthermore, the stars experience a pronounced repulsion along six well-defined, needle-shaped areas (that enclose in a symmetrical way 60^{o}). This highly symmetric energy landscape becomes distorted as we proceed to $\theta = 15^{\text{o}}$: the pronounced maximum in the origin is substantially reduced as the repulsion of the arms is decreased due to the tilting angle. Instead, a rather homogeneous region of repulsion close to the origin (with reddish colours) is observed that extends over a few nm in each direction. For $\theta = 30^{\text{o}}$, this region is characterised by a more pronounced internal structure, with three well-defined, elongated regions (that enclose 120^{o}) along which the stars experience a pronounced repulsion. An increase of θ by 15^{o} leads to a reduction of these repulsions. Eventually, for $\theta = 60^{\text{o}}$, where the two stars are oriented in opposite directions, we can identify three elongated, needle-shaped regions (separated by 120° where the two molecules experience a strong repulsion).

4. Outlook and conclusions

In this contribution, we have calculated the effective potential of charged DNA-stars, i.e., of molecules that are formed by three intertwined ssDNAs: the ensuing, three-armed particles are Y-shaped where each arm consists of 13 base pairs, guaranteeing that the branches can be considered as stiff rods. We assume that these particles are floating as two-dimensional objects on a flat surface that separates two media with possibly different dielectric properties. Based on the charge density along these branches and assuming a potential that quantifies the interaction $\Phi(r)$ between two infinitesimal segments located on two interacting rods, we can derive in Fourier-space a closed expression for the effective potential of two interacting DNA-stars whose centres are connected by a vector $\mathbf{R}$ and which are tilted with respect to each other via an angle θ. Even though the Fourier-transform of the interaction back into real space has to be performed numerically and despite the fact that the resulting potential has to be tabulated on a grid of its three arguments, the total effective interaction is now amenable to be used in computer simulations or theoretical frameworks.

The ensuing effective potential between two interacting DNA-stars shows a complex spatial and orientational dependence. It can, therefore, be expected that an ensemble of interacting DNA-stars will show a highly complex self-assembly scenario.

The model that we have proposed is versatile: (1) the charge density (currently assumed to be constant along the rods which are either infinitely thin or of finite width) can be replaced by a more realistic one, which varies – for instance – spatially along the rod; (2) for the interaction $\Phi(r)$ (currently a screened Coulomb potential) a more realistic potential can be introduced, which reflects the internal architecture of the dsDNA-strands along the rods (see, e.g., [18] or [19]); furthermore, it is desirable (but probably rather intricate) to include volume exclusion interactions among the branches; (3) finally, the interaction potential of active groups, that possibly decorate the tips of the rods can be simply added to the effective potential between two DNA-stars.

Acknowledgements

It is a great pleasure to dedicate this work to Jean-Pierre Hansen, who has made over decades seminal contributions to the liquid state theory and the soft matter theory. Christos N. Likos and Gerhard Kahl express their thankfulness to Jean-Pierre Hansen for many stimulating discussions, for numerous fruitful, scientific cooperations and, in particular, for many years of friendship. Gerhard Kahl acknowledges financial support by the Austrian Science Fund (FWF) under Project Nos. P23910-N16 and F41 – SFB ViCoM. Clara Abaurrea Velasco acknowledges helpful discussions with Marta Montes Saralegui (Wien).

Disclosure statement

No potential conflict of interest was reported by the authors.

Funding

Gerhard Kahl acknowledges financial support by the Austrian Science Fund (FWF) under project numbers [P23910-N16] and [F41] – SFB ViCoM.

References

[1] D.A. Tomalia, A.M. Naylor, and W.A. Goddard, Angew. Chem. Int. Ed. Engl. **29**, 138 (1990).
[2] U. Gupta, H.B. Agashe, A. Ashtana, and N.K. Jain, Biomacromolecules **7**, 649 (2007).
[3] A. D'Emanuele and D. Atwood, Adv. Drug Deliv. Rev. **57**, 2147 (2005).
[4] N.G. Portney and M. Ozkan, Anal. Bioanal. Chem. **384**, 620 (2006).
[5] R.W.J. Scott, O.M. Wilson, and R.M. Crooks, J. Phys. Chem. B. **109**, 692 (2005).
[6] S. Huißmann, C.N. Likos, and R. Blaak, J. Mater. Chem. **20**, 10486 (2010).
[7] S. Huißmann, C.N. Likos, and R. Blaak, Soft Matter **7**, 8419 (2011).
[8] T. Terao, Chem. Phys. Lett. **446**, 350 (2007).
[9] T. Terao, J. Appl. Crystallogr. **40**, 581 (2007).
[10] A. Ohshima, T. Konishi, J. Yamanaka, and N. Ise, Phys. Rev. E **64**, 051808 (2001).
[11] Y.G. Li, Y.D. Tseng, S.Y. Kwon, L. D' Espaux, J.S. Bunch, P.L. McEuen, and D. Luo, Nature Mater. **3**, 38 (2004).
[12] A.A. Kornyshev and S. Leikin, J. Chem. Phys. **107**, 3656 (1997).
[13] A.A. Kornyshev and S. Leikin, Phys. Rev. Lett. **82**, 4138 (1999).
[14] H.M. Harreis, A.A. Kornyshev, C.N. Likos, H. Löwen, and G. Sutmann, Phys. Rev. Lett. **89**, 018303 (2002).
[15] H.M. Harreis, C.N. Likos, and H. Löwen, Biophys. J. **84**, 3607 (2003).
[16] F.H. Stillinger, J. Chem. Phys. **35**, 1584 (1961).
[17] T. Escobar Colla, C.N. Likos, and Y. Levin, J. Chem. Phys. **141**, 234902 (2014).
[18] H.M. Harreis, C.N. Likos, and H. Löwen, Biophys. J. **82**, 3607 (2003).
[19] P.E. Theodorakis, C. Dellago, and G. Kahl, J. Chem. Phys. **138**, 025101 (2013).